



Jenis Artikel: *original research*

Analysis of Audio-Magnetotelluric (AMT) Data Quality Using the Coherence Parameter at Malabar Mountains

Nabila Putri Kusuma¹, Nabilah Rahmawati¹, Shofie Dzakia Hanifah¹, Asep Harja², Gusti Muhammad Lucki Junursyah³

¹Study Program of Geophysics, Faculty of Mathematics and Natural Sciences, Universitas Padjadjaran, Jl. Raya Bandung-Sumedang Km. 21, Jatinangor, 45363

²Department of Geophysics, Faculty of Mathematics and Natural Sciences, Universitas Padjadjaran, Jl. Raya Bandung-Sumedang Km. 21, Jatinangor, 45363

³Center for Geological Survey (CGS), Geological Agency of Indonesia, Ministry of Energy and Mineral Resources, Bandung, 40122

Corresponding e-mail: a.harja@unpad.ac.id

KEY WORDS: audio-magnetotelluric, coherence, noise, skewness

ABSTRACT. Noise recorded during measurements can diminish the quality of AMT data. This can lead to decreased penetration depth and unreliable 1D inversion models. This study aimed to reduce noise and improve data quality by analyzing coherence, curve trend, and skewness. Coherence analysis was performed using robust processing and XPR editing, yielding an average coherence value of 77.5%, an improvement of 10.8% from the raw data. Noise can also alter data dimensionality; hence, skewness analysis was used to determine the effect of distortion on the impedance tensor. Results showed that the 3D dimensionality effect at 6 stations was significantly reduced following coherence and curve trend analyses.

Diterima: 18 June 2024
Direvisi: 29 June 2024
Diterbitkan: 01 July 2024
Terbitan daring: 01 July 2024

1. Introduction

Audio-magnetotelluric (AMT) is a passive geophysical method that utilizes natural electromagnetic waves by measuring perpendicular magnetic and electric fields to determine subsurface resistivity variation (Vozoff, 1972, 1990). AMT refers to the advancement of the MT method fundamental theory was first introduced by Cagniard (1953) and Tikhonov (1950). The AMT method uses a frequency range of 1 Hz to 20 kHz to provide a survey depth range from hundreds of meters to several kilometers (Jiang et al., 2019). This penetration is deeper compared to other electromagnetic geophysical methods such as Ground Penetrating Radar (GPR) and Direct Current (DC resistivity) methods (Erkan, 2008). In recent decades, this method has been widely used in various fields such as oil and gas exploration (Zhang et al., 2014), geothermal exploration (Arafa et al., 2023), and mineral exploration (Jiang et al., 2022). Unfortunately, the natural and wide field sources are uncontrollable and sensitive to electromagnetic noise, including coherent noise caused by natural activity –such as lightning and solar wind– or incoherent noise caused by human activity (Pratiwi et al., 2018). This noise affects data quality and causes an unrepresentative resistivity model that leads to misinterpretation; therefore, noise reduction is needed.

Coherence is an important parameter often used for analyzing data. In general, we can use coherence to estimate the MT impedance to discuss the data quality for a specific period simultaneously (Chen et al., 2022). Coherence refers to a spectral ratio that explains the correlation between perpendicular electric and magnetic fields, which can be expressed mathematically (Mwakirani, 2014):

$$\psi = \frac{(\vec{E} * \vec{H})}{\sqrt{(\vec{E} * \vec{E})(\vec{H} * \vec{H})}} \quad (1)$$

Where ψ is the coherence, \vec{H} is the magnetic field, \vec{E} is the electric field, and * denotes the complex conjugation. Coherence has values ranging from 0 to 1, with 1 indicating the lowest noise contamination and completely coherent signals. However, the \vec{E} and \vec{H} fields will never be fully coherent, as noise will always be present., the minimum requirement coherence value for good-quality AMT data is approximately 0.75 or 75% (Hidayat et al., 2016; Maryani et al., 2016; Widodo et al., 2021).

The survey for this study was conducted around Haruman Peak, Mount Malabar, precisely at Warjabakti Village, Cimaung District, Bandung Regency, with six stations (Figure 1). The Center for Geological Survey (CGS) carried out the survey using the Audio-Magnetotelluric (AMT) method and the instrument MTU-5A Phoenix Geophysics at frequencies from 0.35 Hz to 10400 Hz.

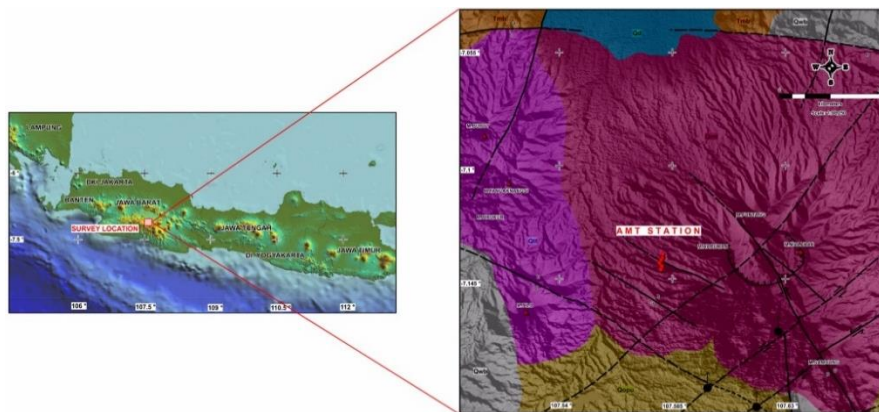


Figure 1. Regional Geological Map of the Survey Location (modified from Bachri et al., 1992)

Mount Malabar is the highest volcano in the mountain group surrounding the Great Bandung Basin. Based on the geological map, the research area is located at the formation in the rock unit of the Malabar-Tilu Volcanics (Qmt), beneath the Undifferentiated Efflata Deposits of Old Volcanics (Qopu), and the Waringin-Bedil Andesite, Old Malabar Formation (Qwb) (Bachri et al., 1992). Malabar mountain is a tropical rainforest with dense

vegetation and high rainfall (Harja et al., 2021). Harja et al. (2023) discovered a shallow and unconfined aquifer at a depth of 40 meters. Based on the morphology and shallow aquifer information from previous research, it is suspected that a deep aquifer zone can be identified using the audio-magnetotelluric method.

Noise in data can also affect its dimensionality, leading to 3D distortion of the magnetotelluric impedance tensor (Chave and Jones, 2012) and reduced depth penetration (Junursyah et al., 2019). The dimensionality of AMT data can be examined using parameter skewness (Swift, 1967). This study aims to improve AMT data quality by analyzing coherence parameters, with additional information from curve trend and skewness analyses. Noise reduction results using coherence analysis can provide qualitative and quantitative information on improving data quality for a more reliable AMT model.

2. Research Methodology

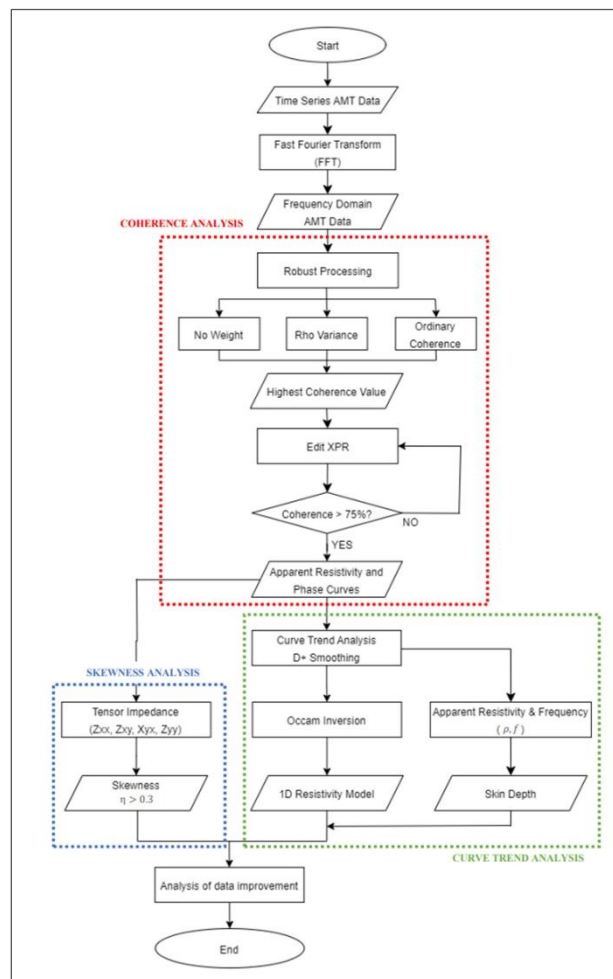


Figure 2. Research Flow Diagram

2.1 Coherence Analysis

The data used in this study are the results of AMT measurements in a time series containing five components of the earth's electromagnetic field measured simultaneously. Fast Fourier Transform (FFT) transforms the time series into the frequency domain. This process is important because some parameters

cannot be analyzed in the time domain (Widodo et al., 2021). The noise reduction process is then performed using the frequency domain's robust and XPR edit processes.

Robust is a statistical estimation using iterative weights of the residual distribution between observations and predictions of the least squares model and provides results resistant to outliers (Chave et al., 1987; Egbert and Booker, 1986; Scheult et al., 1989). Robust processing is also made to simplify and speed up the time needed for manual editing in the XPR edit. There are 3 weighting parameters in this process, which are: (1) No Weight, which weights the data equally at each frequency (it can also be considered raw data); (2) Rho Variance, which weights the data according to its apparent resistivity by giving more weight to the smaller error; and (3) Ordinary Coherence, which weights the data according to its coherence by giving more weight to the higher coherence value. This weighting parameter is critical because it affects the step function in the weighting scheme (Phoenix Geophysics, 2005). The robust results of the three parameters are compared, and the one with the highest coherence value is selected for XPR editing. XPR represents a partial data set combining apparent resistivity and phase values at each frequency divided into 100 partial data. XPR is manually edited by selecting data at frequencies with high average weights and eliminating data with low weights to reduce the effects of noise and minimize outliers so that the trends of the two curves become smoother (Fahrurrozi and Junursyah, 2019).

2.2 Curve Trend Analysis

Curve trend analysis is done manually on the apparent resistivity and phase angle curves from the XPR edit by eliminating the outlier data from the curve trend so that both curves are smoothly aligned with the curve trend by D+ smoothing (Beamish and Travassos, 1992). The data from the curve trend analysis are next analyzed using the skin depth (δ) calculation to confirm the enhanced data quality, which is indicated by the higher skin depth values for deeper penetration depths. Skin depth is defined as the depth in a homogeneous medium where the electromagnetic fields are attenuated to e^{-1} of their amplitudes at the Earth's surface (Simpson & Bahr, 2005). The expression of skin depth can be written as:

$$\delta = \sqrt{\frac{2\rho}{\omega\mu}} = \sqrt{\pi f \mu\sigma} \approx 503 \sqrt{\frac{\rho}{f}} \tag{2}$$

2.3 Skewness Analysis

The dimensionality of magnetotelluric data may be 1-D, 2-D, and 3-D, or it may be because of data processing errors that cause dimensionality changes. Skewness analysis determines if there is any irregularity or telluric distortion in the observed impedance tensor. The phase sensitivity skewness (η) shows the effect of distortion in the impedance tensor and can be mathematically written as follows (Bahr, 1991):

$$\eta = \sqrt{\frac{\text{Re}Z_{xx} \text{Im}Z_{xy} - \text{Re}Z_{yy} \text{Im}Z_{xy} + \text{Re}Z_{xy} \text{Im}Z_{yy} - \text{Re}Z_{yx} \text{Im}Z_{xx}}{|Z_{xy} - Z_{yx}|}} \tag{3}$$

η values above 0.3 can be categorized as the response of the 3-D electric structure below the surface, η values below 0.3 are categorized as the response of 2-D electric structures, while the $\eta = 0$ indicates the ideal 1-D or 2-D structure conditions (Bahr, 1991; Xiao et al., 2011). However, in some cases, values smaller than 0.3 are assumed to represent the responses of a 2D structure (Garcia et al., 1999).

3. Results and Discussion

3.1 Coherence Analysis

Table 1. The result of the Coherence Analysis from 6 stations

STATION	RAW DATA (%)		AVERAGE	ROBUST PARAMETER	ROBUST (%)		AVERAGE	XPR EDIT (%)		AVERAGE
	RHO XY	RHO YX			RHO XY	RHO YX		RHO XY	RHO YX	
MB01	43.4	62.1	52.7	RV	44.5	64.2	54.4	76.2	81.5	78.9

				OC	47.7	66.2	56.9			
MB02	63.1	67.7	65.4	RV	64.4	69.9	67.1	70.6	80.3	75.6
				OC	64.8	69.2	67			
MB03	71.7	75	73.3	RV	72.9	76.7	74.8	76.7	80.3	78.5
				OC	73.4	76.5	75			
MB04	66	69.8	67.9	RV	67	71.2	69.1	74	76.2	75.3
				OC	67.9	71.9	69.9			
MB05	66.1	73.8	70	RV	66.5	74.8	70.6	76.3	82.4	79.4
				OC	68.2	75.9	72.1			
MB06	72.9	69.5	71.2	RV	73.9	70.5	72.2	79.2	76.3	77.8
				OC	73.6	71	72.3			

Data coherence values for raw data, robust processing data, and XPR-edited data are shown in Table 1. The raw data of preliminary AMT measurements at Mount Malabar showed poor quality, with all stations having coherence values $< 75\%$, with the lowest coherence value of 52.7% (MB01) and the highest reaching 73.3% (MB03). After the robust process, the coherence values improved, with four of the five stations showing the best values using the Ordinary Coherence (OC) parameter, with the lowest coherence value of 56.9% (MB01) and the highest reaching 75% (MB03). On average, robust processing only improved the quality of the average coherence value by 1.7%. The coherence value of the XPR edits increased on average by 9.1%, with the lowest coherence value of 75.3% (MB04) and the highest of 79.4% (MB05). Overall, the highest increase in coherence value is at station MB01 by 26.2%, from 52.7% to 78.9%, while the lowest increase is at station MB03 by 5.2%, from 73.3% to 78.5%.

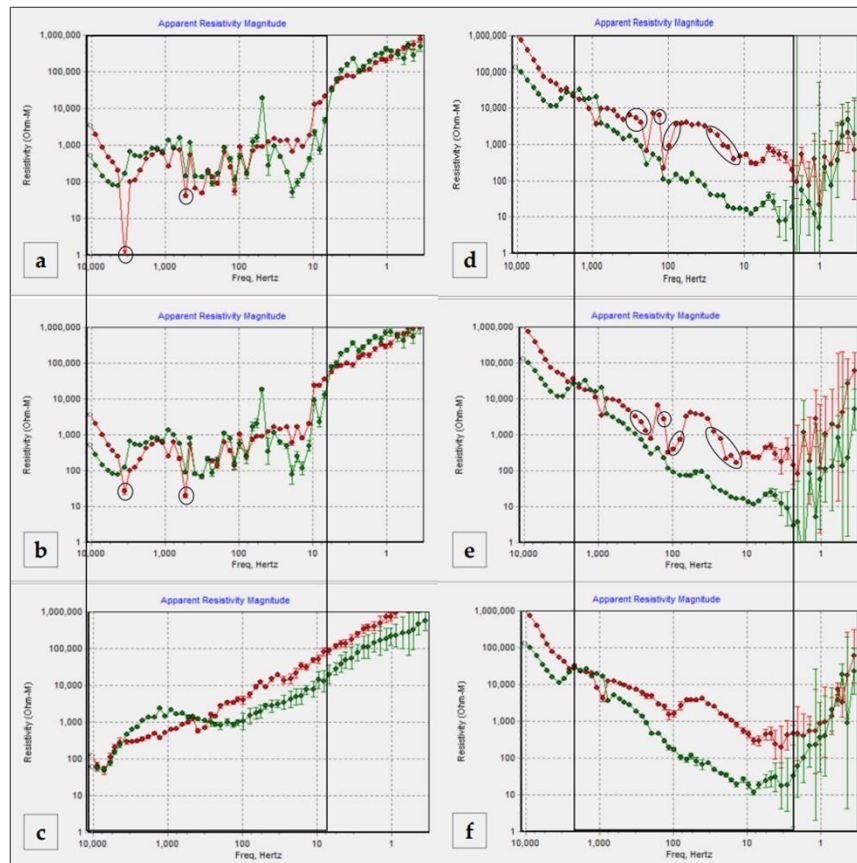


Figure 3. Apparent Resistivity and Phase Curves : (a) MB01 raw data, (b) MB01 after robust, (c) MB01 after XPR Edit, (d) MB04 raw data, (e) MB04 after robust, (f) MB04 after XPR Edit

The apparent resistivity and phase curves show qualitative data quality improvement based on coherence analysis. These are the curves for station MB01, which has the largest increase in coherence that could show a clear contrast in quality, and station MB04, which shows the lowest coherence value of all points indicating a less smooth curve. The increased coherence value is also compatible with the data curves processed with robust and Edit XPR, which appear than the raw data curves. Figure 3 shows that the robust process is not very useful for smoothing the graph, but is highly effective for minimizing the effects of outliers (black circles). This is evident in MB01 curves at frequencies 530 Hz and 3600 Hz, while in MB04 around frequencies 13.7 - 7.5 Hz and 229 - 320 Hz.

3.2 Curve Trend Analysis

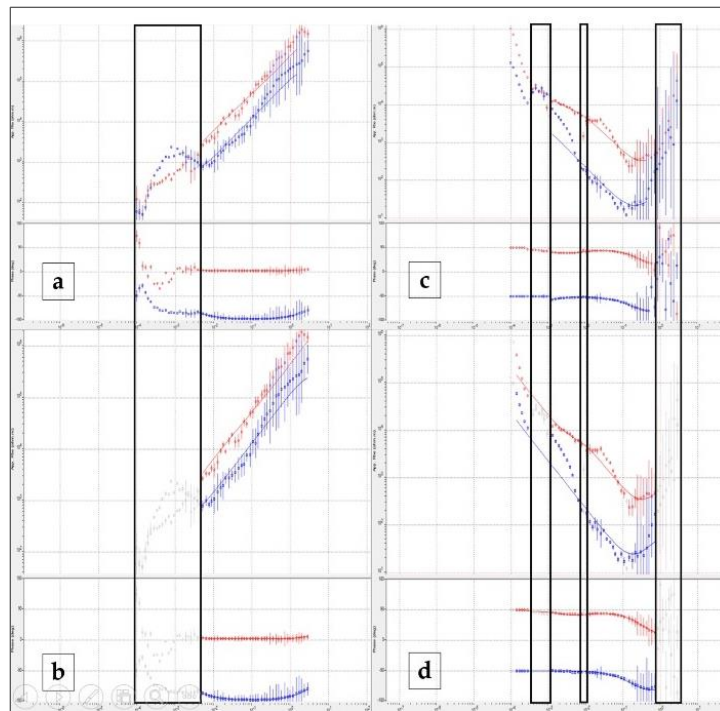


Figure 4. Apparent Resistivity and Phase Curves : (a) MB01 after XPR editing, (b) MB01 after XPR editing based on curve trend, (c) MB04 after XPR editing, (b) MB04 after XPR editing based on curve trend

The results from the coherence analysis can be further validated with the curve trend analysis. This is done by eliminating the points that do not fit the trend. Based on curve trend analysis on data after XPR editing, 17 data were eliminated at MB01 (Figure 4a and 4b) in intervals 0.35 - 0.59 Hz and 229 - 10400 Hz. While at MB04 (Figure 4c and 4d), 15 data were eliminated in the frequency range 0.35 - 1.17 Hz; 115 Hz; 900 - 3000 Hz. The results of the curve trend analysis show a decrease in the amount of data eliminated. The highest amount of data used is at station MB06, 48, and the lowest is at stations MB01 and MB02, 43. The highest increase in the amount of data used is at station MB01, which is 34 data; this is also continuous with the highest rise in coherence value at station MB01 of 26.1%.

Table 2. Total data used based on curve trend analysis in the raw data, robust process, and XPR edit

STATION	TOTAL DATA	DATA USED
---------	------------	-----------

		RAW DATA	ROBUST	EDIT XPR
MB01	60	9	10	43
MB02	60	30	33	43
MB03	60	32	36	46
MB04	60	25	29	44
MB05	60	35	37	46
MB06	60	32	35	48

We can find the average coherence value of 66.8% by utilizing 27 data or eliminating 33 data to see the correlation between curve trend analysis and coherence analysis on raw data. Based on the correlation of coherence analysis in the robust process, we can see the average coherence value of 68.9% by utilizing 30 data or eliminating 30 data. Achieving the best results in the XPR edit process, the correlation of coherence analysis has the most data points of 45 or eliminates 14 data, with the highest average coherence value of 77.5%. These two analyses show that the data contains a lot of noise that cannot be reduced by the robust process alone, especially at station MB01, which only has 10 out of 60 data even after the robust process. The XPR edit proved very effective in reducing noise and can improve the data quality to achieve coherence >75% with eliminated data <20 out of 60 data units.

Table 3. Total data used based on curve trend analysis in the raw data, robust process, and XPR edit

STATION	MAXIMUM SKIN DEPTH (m)		
	RAW DATA	ROBUST	EDIT XPR
MB01	377690	297269	381670
MB02	21381	21519	48183
MB03	9219	13072	48215
MB04	1328	1090	7499
MB05	1318	824	4338
MB06	829	794	3315

Apparent resistivity and frequency from curve trend analysis were then used to determine the penetration depth by using the skin depth (Eq. 2) to validate the quality of AMT data based on coherence analysis. The skin depth process determines the best penetration depth for all data from the curve trend analysis. Based on the skin depth calculation, the average depth for raw data is 4473 m, after robust processing, it is 5976 m, and after XPR editing, it is 18369 m. The shallowest penetration depth reaches 3315 m at MB03, while the deepest penetration depth reaches 381670 m at MB01. We could also see that the robust process reduces the penetration depth at some stations, but showed a major improvement after the XPR editing, aligned with results from coherence analysis.

3.3 Skewness Analysis

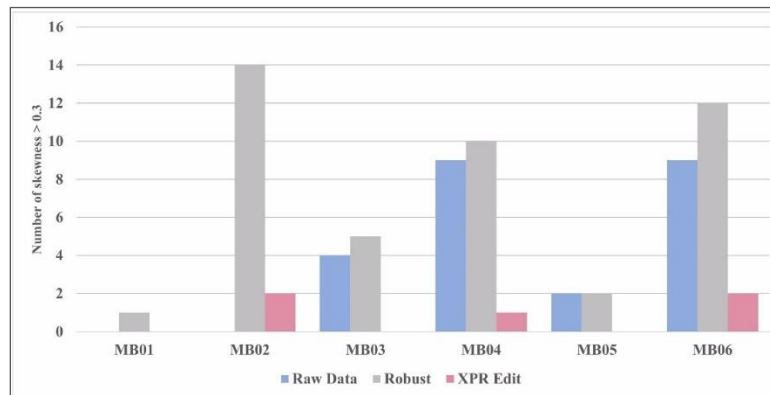


Figure 5. Number of data with a value $\eta > 0.3$

Based on the quantitative skewness analysis of raw data, data after robust, and data after XPR edit (Figure 5), there is a significant difference in reducing the effect of 3D data dimensionality. The value of $\eta > 0.3$ in the raw data is 24, with the highest number found at stations MB04 and MB06. After the robust process, the value of $\eta > 0.3$ instead increased at all stations to 44, with the highest at MB02 (14) and the lowest at MB01 (1). From these results, we can conclude that although robust is sensitive to outliers, it does not smooth out data altogether, so it instead increases the 3D effect. Only after XPR editing, did the 3D effect reduce the value of $\eta > 0.3$ to only 5. MB02 and MB06 had two, MB04 had one, and MB01, MB03, and MB06 had none.

4. Conclusion

The results of coherence analysis using the robust process and XPR editing on AMT data at Mount Malabar, show an increase in coherence value of over 75% at all stations. In each processing, the average coherence value has increased, with details of raw data at 66.8%, robust at 68.9%, and XPR editing at 77.5%, which denotes the greatest average improvement by the XPR edit of 9.1% and 1.7% by the robust process.

The improvement in data quality from the coherence analysis is also evident from the increase in the depth penetration, the increase in data used in the trend curve analysis, and the decrease in the 3D dimensional effect from the skewness analysis. Results of the skewness analysis show that the reduction of 3D dimensionality effects is less effective in the robust process. Qualitatively, the increase in coherence in the robust process does not significantly affect the changes in apparent resistivity and phase curves compared to the raw data. Still, the changes occur notably in the XPR edit process, which shows that the apparent resistivity and phase curves become much smoother.

Acknowledgment

The research was possible thanks to the support of various parties, for which the authors would like to thank the Center for Geological Survey (CGS) for facilitating AMT data acquisition and the entire Malabar AMT survey team for helping during the research. Academic Leadership Grant (ALG) and Riset Kompetensi Dosen Unpad (RKDU) for facilitating this research.

References

- Arafa-Hamed, T., Zaher, M. A., El-Qady, G., Marzouk, H., Elbarbary, S., & Fujimitsu, Y. (2023). Deep heat source detection using the magnetotelluric method and geothermal assessment of the Farafra Oasis, Western Desert, Egypt. *Geothermics*, 109, 102648.
- Bachri, S., Akbar, N., & Alzwar, M. (1992). Peta geologi lembar Garut dan Pameungpeuk, Jawa. Geological map of the Garut and Pameungpeuk Quadrangle, Jawa. In *TA - TT*. Direktorat Geologi Bandung, Indonesia. <https://doi.org/LK>

- <https://worldcat.org/title/715350858>
- Bahr, K. (1991). Geological noise in magnetotelluric data: a classification of distortion types. *Physics of the Earth and Planetary Interiors*, 66(1), 24–38. [https://doi.org/10.1016/0031-9201\(91\)90101-M](https://doi.org/10.1016/0031-9201(91)90101-M)
- Beamish, D., & Travassos, J. (1992). The use of the D+ solution in magnetotelluric interpretation. *Journal of Applied Geophysics*, 29, 1–19. [https://doi.org/10.1016/0926-9851\(92\)90009-A](https://doi.org/10.1016/0926-9851(92)90009-A)
- Cagniard, L. (1953). Basic theory of the magneto-telluric method of geophysical prospecting. *Geophysics*, 18(3), 605–635.
- Chave, A. D., & Jones, A. G. (Eds.). (2012). *The magnetotelluric method: Theory and practice*. Cambridge University Press (CUP). <https://doi.org/10.1017/CBO9781139020138>
- Chave, A., Thomson, D., & Ander, M. (1987). On the robust estimation of power spectra, coherences, and transfer functions. *Journal of Geophysical Research*, 92, 633–648. <https://doi.org/10.1029/JB092iB01p00633>
- Chen, H., Mizunaga, H., & Tanaka, T. (2022). Influence of geomagnetic storms on the quality of magnetotelluric impedance. *Earth, Planets and Space*, 74(1), 111.
- Egbert, G. D., & Booker, J. R. (1986). Robust estimation of geomagnetic transfer functions. *Geophysical Journal International*, 87(1), 173–194. <https://doi.org/10.1111/j.1365-246X.1986.tb04552.x>
- Erkan, K. (2008). A comparative overview of geophysical methods. *Geodetic Science and Surveying*, 3(488), 29–45.
- Fahrurrozi, Z., & Junursyah, G. M. (2019). *The Best 2D Modeling Determination of Magnetotelluric Data in the East Nusa Tenggara and Surrounding Areas Based on Rotational Analysis*.
- Garcia, X., Ledo, J., & Queralt, P. (1999). 2D inversion of 3D magnetotelluric data : The Kayabe dataset. *Earth Planets and Space*, 51, 1135–1143. <https://doi.org/10.1186/BF03351587>
- Harja, A., Aprilia, B. A., & Susanto, D. F. K. (2023). Identifikasi Zona Akuifer Menggunakan Metode Resistivitas-DC di Daerah Kipas Lava Pegunungan Malabar Kabupaten Bandung Jawa-Barat. *Jurnal Ilmu Dan Inovasi Fisika*, 7(1), 49–57. <https://doi.org/10.24198/jiif.v7i1.43216>
- Harja, A., Ma'arif M, F., Nanda, M., Duvanovsky, D., & Shafa, Z. (2021). Studi Hidrogeofisika Gunung Malabar Sebagai Gunung Tertinggi pada Sistem Hidrologi Cekungan Bandung. *Jurnal Geologi Dan Sumberdaya Mineral*, 22, 223. <https://doi.org/10.33332/jgsm.geologi.v22i4.654>
- Hidayat, A., Junursyah, G. M., & Harja, A. (2016). *Analisis deret waktu untuk peningkatan kualitas data magnetotelurik (studi kasus lapangan geothermal)*.
- Jiang, W., Brodie, R., & Duan, J. (2019). Application of audio-magnetotelluric method to cover thickness estimation for drill site targeting. *ASEG Extended Abstracts, 2019*, 1–5. <https://doi.org/10.1080/22020586.2019.12073059>
- Jiang, W., Duan, J., Doublier, M., Clark, A., Schofield, A., Brodie, R. C., & Goodwin, J. (2022). Application of multiscale magnetotelluric data to mineral exploration: an example from the east Tennant region, Northern Australia. *Geophysical Journal International*, 229(3), 1628–1645.
- Junursyah, G. M., Hanif, D., & Mirnanda, E. (2019). *Pengaruh Peningkatan Kualitas Data Magnetotelurik di Pulau Muna dan Sekitarnya Berdasarkan Analisis Koherensi Terhadap Pemodelan 2D*. 5, 49–58.
- Maryani, L., Junursyah, G. M., & Harja, A. (2016). *Analisis Deret Waktu (Time Series) Metode Magnetotelurik Pada Cekungan Buton, Sulawesi Tenggara*.
- Mwakirani, R. M. (2014). *Magneto-telluric (MT) data processing*. <https://api.semanticscholar.org/CorpusID:133792632>
- Phoenix Geophysics. (2005). *Data Processing User Guide Version 3.0*. Phoenix Geophysics Limited.
- Pratiwi, I., Srigutomo, W., & Hidayat, H. (2018). *Data Magnetotelurik Menggunakan Analisis Time series dan Local reference: Studi Kasus Lapangan Shale Gas Kutai*.
- Seheult, A., Green, P., Rousseeuw, P., & Leroy, A. (1989). Robust Regression and Outlier Detection. *Journal of the Royal Statistical Society. Series A (Statistics in Society)*, 152, 133. <https://doi.org/10.2307/2982847>
- Simpson, F., & Bahr, K. (2005). *Practical Magnetotellurics*. <https://doi.org/10.1017/CBO9780511614095>
- Strangway, D. W., Swift, C. M., & Holmer, R. C. (1973). The application of audio-frequency magnetotellurics (AMT) to mineral exploration. *GEOPHYSICS*, 38(6), 1159–1175. <https://doi.org/10.1190/1.1440402>
- Swift, C. (2007). *A Magnetotelluric Investigation of an Electrical Conductivity Anomaly in the Southwestern United States*.
- Tikhonov, A. N. (1950). On determining electrical characteristics of the deep layers of the earth's crust. *Magnetotelluric Methods*, 5, 2.
- Vozoff, K. (1972). The Magnetotelluric Method in the Exploration of Sedimentary Basins. *Geophysics*, 37, 98–141. <https://api.semanticscholar.org/CorpusID:130762518>
- Vozoff, K. (1990). Magnetotellurics: Principles and practice. *Proceedings of the Indian Academy of Sciences - Earth and Planetary Sciences*, 99(4), 441–471. <https://doi.org/10.1007/BF02840313>
- Widodo, A., Lestari, W., Desa Warnana, D., Syaifuddin, F., Rivensky, R., & Ilmawan, R. (2021). Analysis of the effect of magnetotelluric data quality improvement using rho variance and edit XPR parameters in densely populated areas. *IOP Conference Series: Earth and Environmental Science*, 851, 12003. <https://doi.org/10.1088/1755-1315/851/1/012003>
- Xiao, Q., Cai, X., Liang, G., Xu, X., & Zhang, B. (2011). Application of 2D magnetotelluric methods in a geological complex area, Xinjiang, China. *Journal of Applied Geophysics*, 75, 19–30. <https://doi.org/10.1016/j.jappgeo.2011.06.007>
- Zhang, K., Wei, W., Lu, Q., Dong, H., & Li, Y. (2014). Theoretical assessment of 3-D magnetotelluric method for oil and gas exploration: Synthetic examples. *Journal of Applied Geophysics*, 106, 23–36.